*Int. J. Electrochem. Sci.*, 7 (**2012**) 10244 - 10253

International Journal of
ELECTROCHEMICAL
SCIENCE
www.electrochemsci.org

# Germanium Growth in Low Dimensions Based on Relaxed-Porous Silicon by Using A Simple Way of Electrochemical Deposition

*M. J. Jawad*[1], *M. R. Hashim*[1,*], *AND N. K. Ali*[2]

[1]School of Physics, Universiti Sains Malaysia, 11800-Penang, Malaysia
[2]Material Innovations and Nanoelectronics Research Group, Faculty of Electrical Engineering, Department of electronic engineering, Universiti Teknologi Malaysia, 81310 Skudai, Johor, Malaysia
[*]E-mail: mohamed_jassim64@yahoo.com

*Received:* 10 August 2012 / *Accepted:* 11 September 2012 / *Published:* 1 October 2012

---

Porous silicon (PS) technology was used to grow Ge micro-flower on the surface of Si substrates with rough morphology. Low dimensions nanorods were also fabricated directly on the Si substrates through Ge deposition using a simple and low-cost of electrodeposition method for comparison. The characteristics of low dimensions nanorods were investigated for both substrates PS and Si using scanning electron microscopy (SEM), EDX, grazing-angle X-ray diffraction (XRD), and Raman spectra measurements of nanostructures grown on both PS and Si substrate. The texture obtained from SEM images showed that the nanorods were covered by micro-flowers and highly oriented on the porous silicon substrate. Furthermore, the length of nanorods on porous silicon decreased from 10µm to 200 nm and the diameter from 500–200 nm to100 nm. Ge lattice parameters and crystallite size grown on PS and Si were calculated from X-ray diffractograms. It was found that the Ge structures for PS and Si were polycrystalline with a cubic system, whilst the elastic strain on PS was lower than Si substrate. This indicates that Ge on porous lattice is more relax than on silicon. The Raman spectra showed that Ge structure shifted slightly towards to the upper frequency compared with bulk Ge.

---

**Keywords:** Porous silicon, Germanium, Silicon, Strain, nanostructure.

## 1. INTRODUCTION

Over the last two decades, the electronic states in low dimensions structures of group-IV semiconductors like Ge were investigated. Nanocrystals (NCs) of indirect-gap semiconductors, such as Si and Ge are widely studied, as they would open new possibilities for the application of these materials in novel integrated optoelectronics and microelectronics devices. High carrier mobility of Ge grown on strained Si increased the interest of many researchers to study new applications for these

semiconductors. Several techniques are being used to fabricate Ge nanocrystals, such as RF sputtering [1–6], dc sputtering [7], ion implantation [8,9], evaporation–condensation [10], electron beam evaporation [11,12], chemical vapor deposition [13], and pulsed laser deposition [14]. In general, these techniques are expensive and require specialized equipments. Among the above mentioned methods, electrochemical deposition has many advantages such as low-cost, environmentally friendly, high growth rate at relatively low temperatures and easier control of shape and size [15]. The growth of Ge micro-flowers and nanorods arrays through the electrodeposition technique is also possible. However, the mechanism of Ge aligned growth remains an open question and requires further study. Luryi and Suhir reported an interesting calculation showing that Ge on PS could have a lower elastic energy than Ge on Si because porous Si behaves as a sponge-like substrate [16], while, Marty et al. [17] reported that strained–relaxed Ge film has been experimentally grown on porous Si, the TEM results showed that a highly oriented Ge crystal on PS was formed. The idea of this study is to use porous Si as a sponge like substrate, in order to produce a strain-relaxed Ge thin film on a Si substrate. It would be very useful if we could fabricate strain-relaxed Ge/Si without introducing any defects therefore, nano-porous materials used as a template provide a simple way of obtaining Ge in low dimensions. The work on the PS has opened new possibilities for Si-based integrated circuits due to its remarkable optical and electronic properties. Applications of PS, including visible photoluminescence (PL) at room temperature, highly efficient electroluminescent devices, photo detectors, and surface acoustic wave (SAW) devices [18–20]. For comparison purpose, we demonstrate the growth of Ge on a PS surface and on Si at room temperature under identical growth condition morphology and structure of the Ge films were investigated.

## 2. EXPERIMENTAL

### *2.1. Porous Si (PS) preparation*

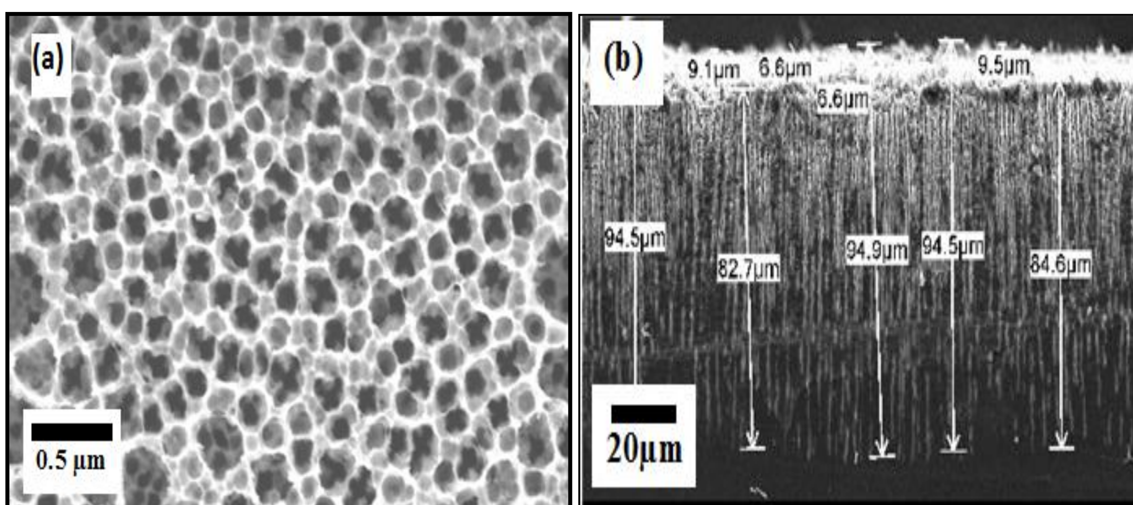


**Figure 1.** (a) SEM image of PS sample and (b) SEM cross section of PS sample prepared at 30 min etching time.

In Fig. 1 porous Si substrate was fabricated by using n-type Si (100) orientation wafer and resistivity of 1-10 Ω cm through the electrochemical anodization method.

In the process, a homemade Teflon cell was used; Si sample and Pt wire were connected as anode and cathode, respectively. The electrolyte was composed of a mixture of 49% aqueous HF and 95% ethanol at a ratio of 1:4 by volume. For the electrochemical etching process, a constant current density of J = 25 mA/cm$^2$ (supplied by a Keithley 220 programmable current source) was used for 30 min. After etching, the samples were rinsed with deionized water and dried in ambient air.

### *2.2. Synthesis of Ge film*

Here we were using a very low cost way to grow Ge thin films our previous work [21]. The method consists of two steps; firstly, the preparation of the solution for Ge electrodeposition by electrochemical etching of Ge target, secondly, the electrochemical deposition of Ge thin film on Si and PS substrates by using the solution extracted from the first step. A piece of Ge sputtering target (99.999% pure, 30 mm × 10 mm × 5 mm) was immersed in a Teflon Beaker containing an electrolyte mixture of HF (49%): $H_2O$ deionized water 1:4. The Ge was connected to the anode via a piece of Pt wire, while another Pt wire was used as a cathode, The current density was 300mA/cm$^2$ (electro-polishing regime) applied for 3 hours. Prior to the PS fabrication and deposition process, the two Si wafers were cleaned using RCA cleaning method. "The RCA clean is a standard set of wafer cleaning steps which needs to be performed before high temp processing steps (oxidation, diffusion, CVD) of silicon wafer involves (organic contaminants, oxides and metallic contaminants removal)". The Si and PS samples were pressed separately to a Teflon cell with an open window fit to wafer. Between the sample and the bottom of cell an *O* ring was used to seal the cell. The sample connected to the cathode and a Pt wire was immersed in the solution as an anode. Two samples were prepared using the same current density 2.5mA/cm$^2$ for one hour. After deposition, the samples were washed several times with deionized water, and dried in ambient air.

## 3. RESULTS AND DISCUSSION

The top-view SEM image of PS sample prepared at 30 min of etching time is presented in Fig. 1(a). For this sample, a uniform distribution of pores around 100~200 nm was observed for PS sample prepared at the optimized condition. The porous network was found to be 85μm as estimated from the SEM cross section as shown in Fig. 1(b). The distribution of the pores is irregular. This could be due to its special feature for the PS which is characterized by a very large internal surface area that induces a large adsorption, and can be regarded as a nanocrystalline skeleton. The growths of Ge films were obtained by a simple and low-cost of electrochemical deposition technique, this method yielded a large area of Ge nanostructures. The entangled Ge nanorods in low dimensions that formed on the Si substrate are presented in Fig. 2 (a) and (b) (smaller scale) as exhibited by SEM images. The lengths of the nanowires were about ten micron and had an average diameter of about 500~200 nm.

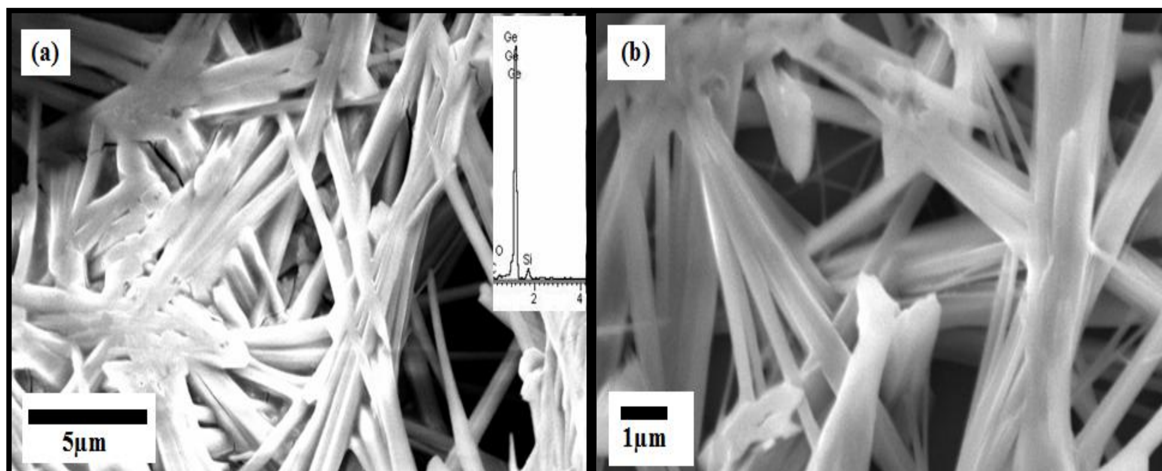


**Figure 2.** (a) Low and (b) high magnification SEM images of Ge nanostructure on Si.

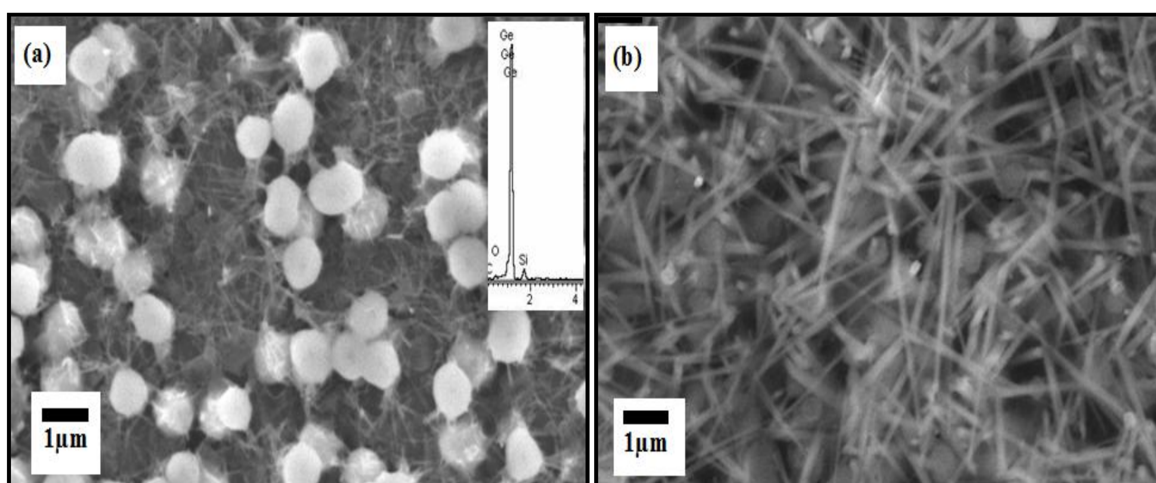


**Figure 3.** (a) Low and (b) high magnification SEM images of Ge micro-flower on PS.

The growth on the PS substrate in lowly magnified image is shown in Fig. 3(a). The distribution of Ge flowers with microstructure of diameter about 0.5µm on whole surface as a cover, while a higher magnification image in Fig. 3(b), shows more details for the net of nanorods under Ge micro-flowers about 100 nm in diameter and their lengths were about 200 nm. The EDX on the top right of Fig. 2(a) and 3(a) confirmed the Ge existence on the substrates.

The average length and diameter of Ge nanorods grown on PS substrate is shorter and thinner than that of grown on Si substrate which can be seen by comparing Fig. 2(b) and Fig. 3(b). This could be due to the rough surface of substrate playing an important role in controlling the initial stage of Ge formation [22]. Due to the applied voltage onto the solution during electrodeposition process, Ge ions will be forced to move toward PS surface. From the SEM images in Fig. 3, the Ge micro-flowers on PS substrate was closely connected with the PS substrate. This could be due to the partial filling of the Ge particles in the pores [23]. Thus, it could improve the structural stability of the porous silicon substrate. The PS surface had a significant effect on the size and shape of the nanorods formed under

micro-flower; thus, there was a decrease in the length and size of the nanorods depending on the roughness of the surface morphology.

To further understand the influence of morphology differences on the properties of Ge structures, XRD was used to study the crystalline structure and distribution of the products, Fig. 4 illustrates the typical XRD pattern of the Ge nanorods grown on Si and Ge micro-flowers on PS, all the observed diffraction peaks well agreed with the standard card of bulk Ge with a cubic structure.

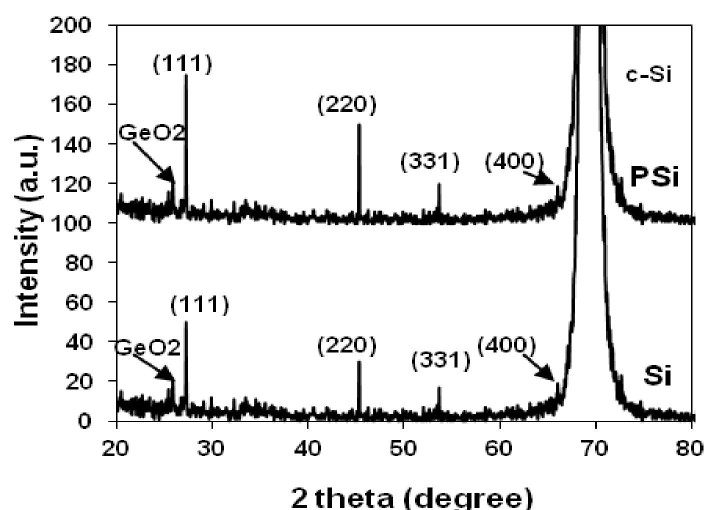


**Figure 4.** XRD spectra of Ge structures grown on Si and PS

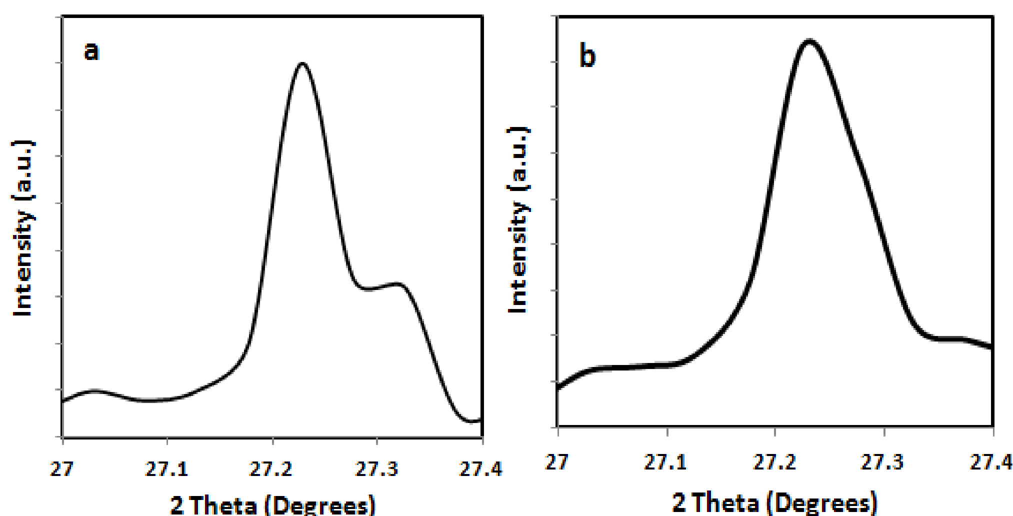


**Figure 5.** Enlarged XRD peak of Ge at (111) orientation (a) Ge/Si and (b) Ge/PS (Si).

Moreover, the as grown Ge structures were polycrystalline in nature with a cubic system. The diffraction patterns were represented by several peaks appeared in the spectra of Ge films at (111), (220), (311), and (400) within 2θ from 20° to 80°. These peaks are reflected from both Si and PS

surfaces which correspond to Ge(c-Ge) [24], the dominant peak at 2θ = 69.24° is the (400) diffraction from c-Si substrate [25], the films show a sharp peak centered at about 26°, which is attributed to presence of hexagonal $GeO_2$ peak [26], it can also be seen that for the Ge micro-flowers on PS substrate the intensity of the (111) oriented peak at 27.28° was the strongest and three times turn to be higher than on Si substrate.

Figure 5 shows that the XRD peaks enlarged for the Ge at mean peak of (111) orientation for two samples. The figure reveals that the Ge grown on PS (Si) (fig. 5b) is free from the impurities compared to that grown on Si (fig. 5a) also, the spectrum of Ge/Si showed the long tail at the right side of the peak which could be due to the deformation of Ge crystal lattice from intrinsic stress introduced by impurities and defects in the crystal while, the sample grown on PS has broader full width at half maximum (FWHM), compared to other sample. Furthermore, the strong intensity and narrow Ge diffraction peaks also indicated that the resulting products had good crystallinity, while, peaks at (220), (311), and (400) indicated that nonepitaxial growth occurred (fig. 4).

Bragg's law can be used to obtain the lattice spacing of a particular cubic system through the following relation:

$$d = \frac{a}{\sqrt{h^2 + k^2 + l^2}} \qquad (1)$$

Where $d$ is the lattice spacing of the cubic crystal, $a$ is lattice constant and $h$, $k$, and $l$ are the Miller indices of the Bragg plane, so that, the lattice constants of Ge films can be calculated by using d-spacing values for plane (111) as shown in Table 1.

**Table 1.** Lattice parameters for bulk Ge and Ge films samples corresponding to plane (111)

| Sample | d ($\overset{\circ}{A}$) | $a = b = c$ ($\overset{\circ}{A}$) | FWHM [°2Th.] | $D$ (nm) |
|---|---|---|---|---|
| Bulk Ge | 3.26593 | 5.6568 | | |
| Ge/Si | 3.27429 | 5.7011 | 0.2952 | 27 |
| Ge/PS | 3.27158 | 5.6889 | 0.3600 | 22 |

The result showed crystallographic parameters: $a = b = c$, (cubic crystal) appeared to be relatively consistent with actual values of bulk Ge [27], while, the average crystallite size of the Ge nanostructures can be estimated by the Scherrer formula using the full width at half-maximum (FWHM) value of the XRD diffraction peaks:

$$D = \frac{0.9\lambda}{\beta COS\theta} \qquad (2)$$

Where $D$, $\lambda$, $\theta$ and $\beta$ are the crystallite size, X-ray wavelength of 0.154 nm, Bragg diffraction angle (27.2365°), and the parameter ($\beta$) can be calculate by the FWHM. The values of $D$ obtained

were about 22 nm for micro-flower on the PS substrate and 27 nm for nanorods on Si substrate. The values indicated that the pore size of the PS has a significant effect on the mechanism of synthesis of Ge in low dimensions. This could be the initial point of growth of the nanostructures, which starts from the center of the pore and spreads to form the micro-flower. The strained lattice parameters ($\varepsilon_a$) of the Ge structure from the lattice parameter ($a$) of the Ge on Si and Ge on PS can also be determined as shown in Table 2, which are different from the bulk lattice parameter values ($a_o = 5.6568\,\mathring{A}$) [27].

**Table 2.** Lattice parameters and strain determined for the Ge samples

| Sample | $a\,(\mathring{A})$ | $\varepsilon_a$ (%) |
|---|---|---|
| Ge/Si(100) | 5.7011 | 0.783 |
| Ge/PS(100) | 5.6889 | 0.567 |

The elastic strain, $\varepsilon_a$ of Ge films is also listed in the Table 2, calculated from the following relation [28].

$$\varepsilon_a = \frac{\Delta a}{a_0} \tag{3}$$

where ($\Delta a$) is defined as the deviation of the calculated lattice parameter ($a$) from the corresponding unstrained values $a_o$.

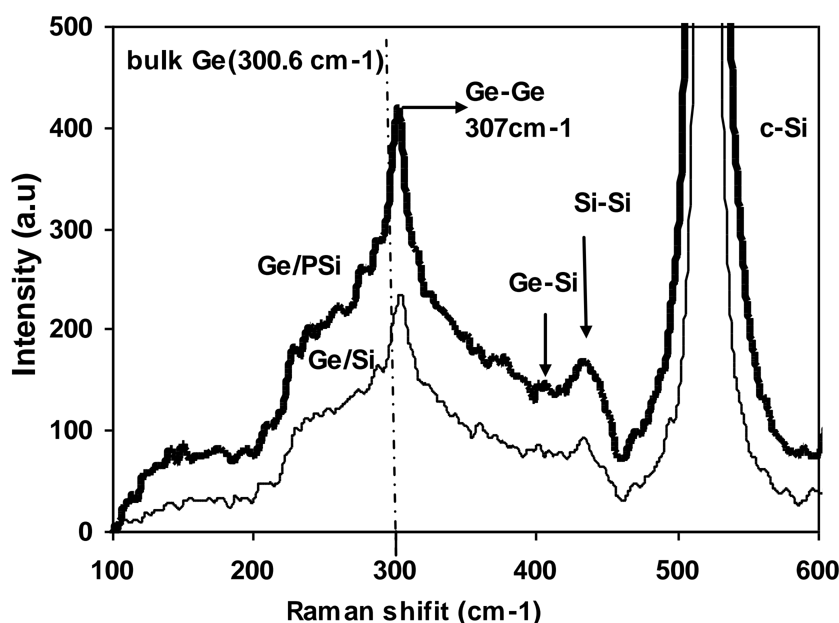


**Figure 6.** Typical Raman spectrum comparing Ge-Ge mode for Ge/PS, Ge/Si samples with bulk Ge.

The positive value of the in-plane strain $\varepsilon_a$ indicates that the strain caused by the substrate is tensile, on the other hand; the results showed Ge on porous had a lower elastic strain than Ge on Si [29], therefore, the rough surface morphology of the PS substrate plays a major role in controlling the growth of the Ge layer. The porous layer is a good substrate to reduce lattice mismatch hetero-structure due to its special surface morphology [30]. The vibrational spectra of the samples were studied using Raman scattering spectroscopy excited by a 488 nm laser line. Fig. 6 shows the Raman spectra from the two samples, indicating the shift of the phonon modes for these samples as compared with phonon frequency of a bulk Ge (300.6 $cm^{-1}$)[27].

A typical Raman spectrum of the Ge/Si and Ge/PS are the strong peaks at 521 $cm^{-1}$ could be due to the Si phonon mode from the c-Si substrate [31], while, the peaks in both cases located at 307 $cm^{-1}$ could be attributed to the optical phonon contribution of the Ge-Ge stretching mode. The peaks were blue shifted by ~6 $cm^{-1}$ as compared to that of bulk Ge; such a shift may be caused by mechanical stresses in Ge clusters [32]. The 307 $cm^{-1}$ peak is the signature for existence of Ge nanocrystals with cubic structure, on the other side, a very weak 410 $cm^{-1}$ peak represents the occurrence of Ge–Si bonds whilst 440 $cm^{-1}$ peak resulted from Si–Si bonds [33, 34]. After starting the deposition process of Ge ions on the surfaces of PS and Si, Si–Si optical phonons are localized in the Ge neighborhoods. Many Si–O bonds in the surface of PS were destroyed and some Ge, Si, and O ions were produced [33].

## 4. CONCLUSION

In summary, large-scale aligned Ge micro-flowers in low dimensions and nanorods on PS and Si using a simple technique of electrochemical deposition of Ge were synthesized at room temperature. The dependence of the structural of low-scale structures on different substrates were investigated systematically. SEM exhibited that the Ge nanorods formed on PS were shorter and thinner than Ge formed on Si. However, the nanostructures of Ge formed on PS and Si surfaces were polycrystalline in nature, and the highest oriented plane was (111) which showed cubic crystal. The calculated lattice parameters were close to actual values of bulk Ge. It was also noted that the crystallite size of Ge on porous was smaller than Ge on Si beside stronger emission intensity and the smaller FWHM for Ge micro-flowers obtained on PS substrate compared to Ge nanorods as grown on Si substrate, furthermore, evaluated elastic strains for both Ge/PS and Ge/Si layers using XRD demonstrated that PS was strained and Ge on PS had lower strain than Ge on Si. The Raman spectra from the two samples also show slightly blue shifted relative to bulk Ge indicating mechanical stresses in the sample.

ACKNOWLEDGEMENT
The authors would like to thank the financial assistance provided by Universiti Sains Malaysia, Penang.

**References**

1. Y. Maeda, *Phys. Rev. B*, 51 (1995) 1658.
2. A.G. Rolo, M. I. Vasilevskiy, O. Conde and M. G. M. Gomes, *Thin Solid Films*, 336 (1998) 58.
3. W. K. Choi, S. Kanakaraju, Z. X. Shen and W. S. Li, *Appl. Surf. Sci.*, 145 (1 999) 697.
4. Y. W. Ho, V. Ng, W. K. Choi, S. P. Ng, T. Osipowicz, H. L. Seng, W. W. Tjui and K. Li, *Scr. Mater*, 44 (2001) 1291.
5. Y. X. Jie, A. T. S. Wee, C. H. A. Huan, W. X. Sun, Z. X. Shen and S. J. Chua, *Mater. Sci. Eng. B* 107 (2004) 8.
6. S. K. Ray and K. Das, *Opt. Mater.*, 27 (2005) 948.
7. M. Zacharias and P. M. Fauchet, *J. Non-Cryst. Solids*, 227–230 (1998) 1058.
8. C. Bonafos, B. Colombeau, A. Altibelli, M. Carrada, G. Ben Assayag, B. Garrido and M. Lopez, *Nucl. Instrum. Methods Phys. Res. B*, 178 (2001) 17.
9. K. Masuda, M. Yamamoto, M. Kanaya and Y. Kanemitsu, *J. Non-Cryst. Solids*, 299–302 (2002) 1079.
10. A. Stella, P. Tognini, C. E. Bottani, P. Milani, P. Cheyssac and R. Kofman, *Thin Solid Films*, 318(1998) 100.
11. Q. Wan, C. L. Lin, N. L. Zhang, W. L. Liu, G. Yang and T. H. Wang, *Appl. Phys. Lett.*, 82 (2003) 3162.
12. Q. Wan, C. L. Lin, W. L. Liu and T. H. Wang, *Appl. Phys. Lett.*, 82 (2003) 4708.
13. Z. He, J. Xu, W. Li, K. Chen and D. Feng, *J. Non-Cryst. Solids*, 266–269 (2000) 1025.
14. Y. Zhu and P. P. Ong, *J. Phys. Condens Matter*, 13 (2001) 4075.
15. H. Ishizaki, M. Imaizumi, S. Matsuda and M. Izaki, *Thin Solid Films*, 411 (2002) 65.
16. Luryi, Serge and Suhir, Ephraim, *Appl. Phys. Lett.*, 49 (1986) 140.
17. O. Marty, T. Nychyporuk. J. De La Torre, V. Lysenk, G. Bremond and D. Barbier, *Appl. Phys. Lett.*, 88 (2006) 101909.
18. Z. Gaburro , P. Bettotti, M. Saiani , L. Pavesi, L. Pancheri , C. J. Oton and N. Capuji, *Appl. Phys. Lett.*, 85 (2004) 555.
19. S. E. Lewis, J. R. Deboer, J. L. Gole and P. J. Hesketh, *Sens. Actuators B*, 110 (2005) 54.
20. V. M. Aroutiounian, K. h. Martirosyanl and P. Soukiassian, *J. Phys. D: Appl. Phys.*, 37 (2004) L25–L28.
21. M. J. Jawad, M. R. Hashim, N. K. Ali,b, E. P. Corcoles and M. E. Sharifabad, *Journal of The Electrochemical Society*, 159 (2012) D1-D5.
22. H. I. Abdulgafour, F. K.Yam, Z. Hassan, K. AL-Heuseen and M. J. Jawad, *Journal of Alloys and Compounds*, 509 (2011) 5627.
23. C. Fang, E. Foca, L. Sirbu, J. Carstensen1, H. Foll and I. M. Tiginyanu, *phys. stat. sol. (A)*, 204 (2007) 1388.
24. A. G. Rolo, O. Conde, M. J. M. Gomes and M. P. Dos Santos, *Journal of Materials Processing Technology*, 92-93 (1999) 269.
25. A. Suzuki and M. Isomura, *J. Non-Cryst. Solids*, 32 (2011) 489.
26. S. Guha, M. Wall and L. L. Chase, *Nucl. Instr. and Meth. in Phys. Res. B*, 147 (1999) 367.
27. G. C. Van de Walle and R. M. Martin, *Phys. Rev. B*, 34 (1986) 5621.
28. J. Krüger, G. S. Sudhir, D. Corlatan, Y. Cho, Y. Kim, R. Klockenbrink, S. Rouvimov, Z. Liliental-Weber, C. Kisielowski, M. Rubin, E. R. Weber, B. McDermott, R. Pittman and E. R. Gertner, *Mater. Res. Soc. Symp. Proc.*, 482 (1998).
29. N. Usami, K. Kutsukake, K. Nakajima, S. Amtablian, A. Fave and M. Lemiti, *Appl. Phys. Lett.*, 90 (2007) 031915.
30. H. Caia, H. Shen, Y. Yin, L. Lu, J. Shen and Z. Tang, *J. Phys. Chem. Solids*,70 (2009) 967.
31. X. L. Wu and Y. Gu, *J. Appl. Phys.*, 86 (1999) 707.

32. K. Das, S. P. Mondal, A. Dhar and S. K .Ray, *Pro. of the 14th International Workshop on the Physics of Semiconductor Devices, IWPSD,* art. no. 4472524 (2007) 377.
33. X. L. Wu, T. Gao, X. M. Bao, F. Yan, S. S. Jiang and D. Feng, *J. Appl. Phys*., 82 (1997) 2704.
34. P. D. Persans, A. F. Rupper, B. Abeles and T. Tiedje, *Phys. Rev. B*, 32 (1985) 5558.

© 2012 by ESG (www.electrochemsci.org)